Effects of Ionizing Radiation on Crystalline Cytosine Monohydrate

Stacey D. Wetmore,[†] Fahmi Himo,[‡] Russell J. Boyd,[†] and Leif A. Eriksson*[,‡]

Department of Chemistry, Dalhousie University, Halifax, B3H 4J3 Nova Scotia, Canada, and Department of Physics, Stockholm University, Box 6730, S-113 85 Stockholm, Sweden

Received: March 31, 1998; In Final Form: July 1, 1998

Possible radical reaction products observed when subjecting monohydrate crystals of the DNA base cytosine to ionizing radiation are characterized and analyzed by means of density functional theory. Comparison is made with data from a recently published detailed ESR and ENDOR study by Sagstuen et al. (Sagstuen, E.; Hole, E. O.; Nelson, W. H.; Close, D. M. *J. Phys. Chem.* **1992**, *96*, 8269), as well as earlier studies on methylcytosine and cytidine monophosphates. For cytosine monohydrate it is found, when comparing computed and measured radical hyperfine coupling constants, that products other than those initially assumed are possibly being formed. Instead of the original model that irradiation leads to the net reaction of dehydrogenation at the N1 position of one cytosine molecule and hydrogenation at the N3 position of a second cytosine, we present an alternative mechanism where water is involved in the process. This alternative mechanism leads to the formation of N3 hydrogenation and C5 hydroxylation net products, as the main reactions. Not only do the hyperfine couplings provide a better match for the latter but they are also energetically favored over the first mechanism.

Introduction

Radiation damage to DNA has gained significant attention during recent decades owing to the effects caused by depletion of stratospheric ozone and the concomitant increase of UV radiation, as well as in the use of radiation therapy in, for example, cancer treatment. Several experimental studies are available of radicals resulting from radiation damage to DNA—both on full DNA samples and on model systems.[1−5] Radiation to DNA is known to generate a multitude of base-centered radicals, which then may react/rearrange within the DNA sample and eventually lead to cleavage of the DNA strand. Other observed reactions are the creation of σ-bonds between DNA bases as observed for, e.g., thymines,[6,7] or that a base radical reacts with a nearby protein to form, e.g., thymine−tyrosine links.[2,8−10] Still, however, relatively little detailed knowledge exists regarding the exact reaction mechanisms, and to some extent even in what form (neutral, charged, adducts, ...) the radicals are created.

Relatively few accurate theoretical studies of DNA base radicals are available, primarily owing to a lack of appropriate methods to deal with such large systems at high accuracy. Colson and Sevilla have recently reviewed results from ab initio HF and MP2 calculations of primarily electron affinities, ionization potentials, and excited states of DNA bases, as well as effects of base−water interactions.[11] Paglieri et al.[12] have investigated different cytosine and uracil tautomers in the gas phase and upon the inclusion of solvent interactions. Hutter and Clark[13] and Sponer and Hobza[14] have recently conducted studies of the G−C base pair radical cation and of the amino group dihedral angle modifications upon base pair formation, respectively. The three latter studies were conducted within the framework of novel density functional theory (DFT). DFT has over the past few years proven to be the most cost-effective method presently at hand, as it allows for studies of realistically large model systems, at a correlated level.[15,16] In our laboratory, we have recently initiated a series of studies of model radical systems of biophysical interest, such as amino acid, quinone, and DNA base radicals,[17−23] as well as full enzymatic reaction mechanisms[24] and interprotein radical transfer processes.[25] Owing to the many problems associated with experimental work on these types of material, from sample preparation to analysis/interpretation, and the apparent success of current DFT methods in reproducing experimentally measured quantities, it is becoming increasingly evident that theoretical calculations have an important role in the understanding of processes in biological systems.

We herein present results from theoretical (DFT) studies of possible radical products formed by irradiation of the DNA base cytosine. To ensure that comparison is made with cytosine radicals only, our analysis is based primarily on experimental ESR and ENDOR studies of crystalline samples of cytosine monohydrate at 10 K, performed by Sagstuen et al.,[26] rather than on studies of full DNA chains. The crystal structure of cytosine monohydrate has been determined to high resolution, and it has been shown that the cytosines are connected to each other and to the water molecules through a network of hydrogen bonding.[27] From spectral simulations, Sagstuen et al.[26] concluded that two major radical products, at 38−47% yield each, were formed when the crystalline sample was subjected to ionizing radiation accompanied by several other radicals produced at low yields. The main products were interpreted as the neutral N1 dehydrogenated and N3 hydrogenated radicals, respectively (cf. Scheme 1). To make a full analysis of the reaction products, we have optimized geometries and computed relative energies and radical hyperfine structures of all possible neutral hydrogenation, dehydrogenation, and hydroxylation products of cytosine (C), as well as its radical anion and cation. Comparison is also made, where applicable, to experimental ESR and ENDOR data for crystalline 1-methylcytosine (1MeC),[28]

[†] Dalhousie University.
[‡] Stockholm University.

S1089-5647(98)01691-5 CCC: $15.00
Published on Web 08/26/1998

SCHEME 1

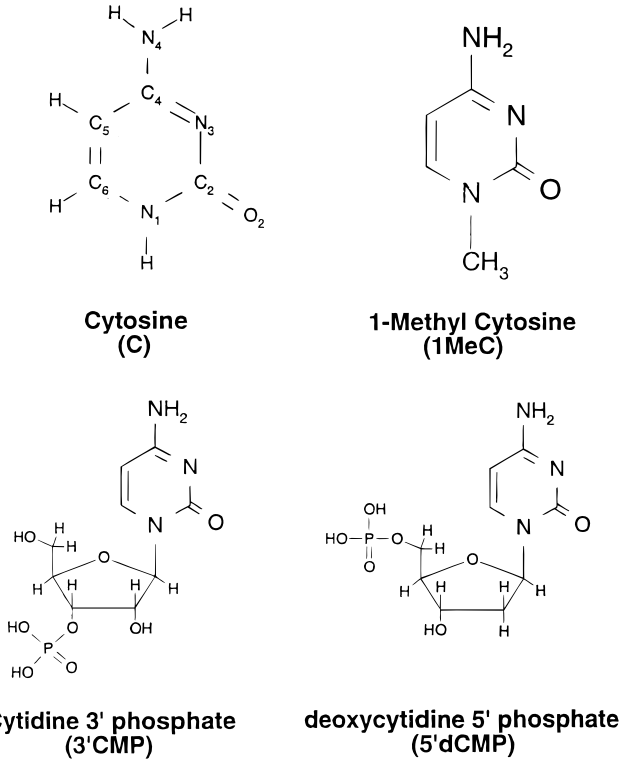

cytidine 3′-monophosphate[29] (3′CMP), and deoxycytidine 5′-monophosphate (5′dCMP),[30] depicted in Scheme 1.

Theoretical Approach

All systems reported in this work are geometry optimized using the hybrid Hartree−Fock-DFT functional B3LYP in conjunction with the 6-31G(d,p) basis set. The functional consists of a linear combination of HF exchange, Slater's local exchange,[31] and Becke's 1988 gradient correction thereof,[32] combined with the Vosko−Wilk−Nusair local[33] and Lee−Yang−Parr gradient-corrected correlation contribution.[34] The relative weights were determined by Becke[35] (although using a different correlation functional than "LYP") from a least-squares fit to atomization energies, ionization potientials, and electron affinities. Frequency calculations at the same level of theory were performed to ensure that the optimized structures were local minima on the potential energy surfaces. Albeit zero-point vibrational energies (ZPE) were thereby obtained, these were not included in the final energetics (see below)—for the most part we compare relative energies within the same group of radicals (OH adducts, dehydrogenated species, etc), for which the differences in ZPE are within 1 kcal/mol.

Single-point calculations were subsequently carried out at the B3LYP/6-311G(2df,p) level to determine relative energies and at the PWP86/6-311G(2d,p) level for isotropic and anisotropic hyperfine coupling constants (HFCCs). The latter is a "pure" DFT functional and uses the gradient correction to the local exchange by Perdew and Wang[36] and to the correlation by Perdew.[37] B3LYP calculations are conducted with the program suite Gaussian 94,[38] and the PWP86 calculations with the deMon code,[39] using the (5,4;5,4) family of auxiliary basis sets for the fitting of the charge density and the exchange correlation potential. The present combination of methods has previously been employed in studies of, e.g., histidine radicals,[20] quinone radicals,[21] and model π-radicals[40] and has been found to yield results of very high accuracy. In particular, it has been noted that the isotropic HFCCs are more accurate at this level (PWP86/6-311G(2d,p)) than employing the corresponding B3LYP functional.[40] The isotropic HFCCs are obtained by considering the unpaired spin density at the nucleus in question

$$A_{iso} = (8\pi/3)g\beta g_N\beta_N\rho^{\alpha-\beta}(0)$$

where g and β are the electronic g-factor (generally assumed to the free electron value, 2.0023) and the bohr magneton, respectively, and g_N and β_N are the corresponding nuclear factors for nucleus N. For the anisotropic components, the density of unpaired spin at $r = 0$ is replaced by the corresponding dipole−dipole integrals, rendering the diagonal elements (xx, yy, zz) of the 3×3 anisotropic HFCC tensor. For more details about the calculations of hyperfine coupling constants and performance of different DFT functionals, we refer to, e.g., refs 41−43.

The optimized geometries are not reported in this work but may be obtained from the authors. Throughout the paper, experimentally assigned conformers are given within quotation marks, whereas theoretically determined results are referred to using boldface (e.g. "N3H" and **N3H**).

Previous ESR/ENDOR Data for Cytosine Derivatives

In Table 1 we review the experimentally measured HFCCs observed in irradiated cytosine derivatives and their original assignments.[26,28−30] As discussed above, the original proposal regarding the net radiation products in cytosine monohydrate is that a hydrogen atom (or, rather, ionization followed by deprotonation) is removed from the N1 position of one cytosine and added to the N3 position of a second cytosine unit. This leads to a radical center at the C5 position for the "N1" dehydrogenated radical, and a C6-centered radical for the "N3H" hydrogen adduct. The main hyperfine components were assigned to the C5 and the two amino group protons, and to the C6, N3, and one amino group proton for the two cases, respectively. On the basis of the McConnell relation and various empirical Q-values, π-spin densities of 0.52 (C6), 0.07 (N3), and 0.06 (N4) were estimated for the "N3H" species, and 0.58 (C5), 0.17 (N4), and 0.30 (N1 or N3) for the "N1" radical. Since in this work the total ($\pi + \sigma$) spin densities are calculated and the H or OH addition products can no longer be regarded as "pure" π-systems after the creation of an sp^3-hybridized center in the ring, a direct comparison is really not feasible. However, the estimated values will provide some indication of the validity of the approach. At room temperature, Herak et al.[44] reported an additional radical assigned to the "O2H" hydrogen adduct. In 1-methylcytosine, three radical species have been reported,[28] ascribed to the two hydrogenation adducts at C5 and C6 and the N3 protonated radical anion, respectively. The latter is observed upon cocrystallization with 5-fluorouracil.

For the larger cytosine derivatives, we employ data sets for two systems, cytidine 3′-monophosphate[29] and deoxycytidine 5′-monophosphate,[30] in our comparisons. In 3′CMP, the radical observed was originally proposed by Box et al.[29] to arise from the anion, an assignment that later has been questioned by Close[5] in favor of the "N3H" adduct. Close and Bernhard studied the radiation products of 5′dCMP monohydrate crystals at 6 K.[30] They observed two main cytosine-centered products after irradiation, which were assigned to the radical cation (protonation state unknown) and the "N3H" adduct, respectively. The HFCCs for these radicals are listed in Table 1. One of the observed proton couplings of the "radical cation" in 5′dCMP was ascribed to the β-proton on the C1′ carbon connecting the cytosine to the sugar ring. They also reported a joint N1 + N3

TABLE 1: Experimental Hyperfine Coupling Constants (MHz) Observed in Cytosine Monohydrate,[26] 1-Methylcytosine,[28] Cytidine-3′-phosphate Hydrate,[29] and Cytidine-5′-phosphate Monohydrate[30]

system	radical	HFCC	N3−H	N4−Ha	N4−Hb	C5−H	C6−H	HX
C	"N1"	A_{iso}		−14.3	−13.0	−41.4		
		T_{xx}		−9.3	−6.2	−21.0		
		T_{yy}		−1.8	−3.6	−0.8		
		T_{zz}		11.1	9.7	21.8		
	"N3H"	A_{iso}	−5.5	−4.5			37.8	
		T_{xx}	−5.8	−4.7			−24.7	
		T_{yy}	−1.5	−2.2			2.3	
		T_{zz}	7.2	6.8			22.4	
	"C5H"	A_{iso}				132[a]	−52.4	87[a]
		T_{xx}					−31.6	
		T_{yy}					−1.5	
		T_{zz}					30.2	
	"C6H"	A_{iso}				−51.8		
		T_{xx}				−28.2		
		T_{yy}				−0.1		
		T_{zz}				28.3		
	not assigned	A_{iso}					−51.1	
		T_{xx}					−26.8	
		T_{yy}					2.5	
		T_{zz}					24.2	
1MeC	"N3H"	A_{iso}					−38.6	
		T_{xx}					−23.9	
		T_{yy}					4.0	
		T_{zz}					19.9	
	"C5H"	A_{iso}				126.5	−48.8	86.2[b]
		T_{xx}				−4.3	−32.3	−3.8
		T_{yy}				−3.2	2.6	−3.4
		T_{zz}				7.5	29.6	7.2
	"C6H"	A_{iso}				−49.9	133.7	143.7[c]
		T_{xx}				−30.0	−5.9	−4.0
		T_{yy}				3.0	−2.6	−2.5
		T_{zz}				27.0	8.5	6.5
5′dCMP	"cation"	A_{iso}				−42.2		41.6[d]
		T_{xx}				−21.3		−2.8
		T_{yy}				−2.5		−1.2
		T_{zz}				23.9		4.0
	"N3H"	A_{iso}					−39.1	
		T_{xx}					−24.4	
		T_{yy}					5.8	
		T_{zz}					18.5	
3′CMP	"anion"	A_{iso}					−36.0	
		T_{xx}					−23.3	
		T_{yy}					2.0	
		T_{zz}					21.3	

[a] Only isotropic components reported. [b] Hydrogen atom added to C5. [c] Hydrogen atom added to C6. [d] β-coupling at the C1′ sugar ring carbon.

^{14}N hyperfine tensor of (42.7, 17.3, 0.3) MHz, with the isotropic couplings for the two nitrogens being 7 and 14 MHz, respectively. In 5′dCMP, no "N1" dehydrogenated product is possible owing to the connecting sugar ring. However, the couplings for the C5−H proton of the cationic radical in this system are very similar to those observed by Sagstuen et al. in cytosine monohydrate, assigned to the "N1" dehydrogenation product. This may indicate that there is reason to reinvestigate the assignment of the **N1** radical in cytosine.

Theoretical Results

A. Charged Cytosine Radicals. In Table 2, we list the computed full hyperfine tensors for the optimized cation and anion radicals of cytosine. The adiabatic ionization potential, computed at the B3LYP/6-311G(2df,p) level on the B3LYP/6-31G(d,p) optimized structures, is 8.42 eV. This compares well with the corresponding experimental data of 8.37 eV[45] and the data reported by Colson and Sevilla[11] obtained at the MP2/6-31+G(d)//6-31G(d) level (8.43 eV). The adiabatic electron affinity is determined to be rather high, 0.57 eV.

TABLE 2: Computed Proton HFCCs (MHz) and Energetics (eV) for the Cytosine Radical Cation and Anion

radical	HFCC	N1−H	N4−Ha	N4−Hb	C5−H	C6−H
cation IP = 8.42	A_{iso}	−10.8	0.7	0.7	−22.6	−1.3
	T_{xx}	−5.9	−2.2	−1.9	−13.3	−2.8
	T_{yy}	−4.6	−1.5	−1.3	−1.6	−1.9
	T_{zz}	10.4	3.6	3.1	14.9	4.8
anion EA = −0.6	A_{iso}	5.9	5.5	11.8	−1.1	0.8
	T_{xx}	−9.6	−2.5	−2.6	−4.1	−22.3
	T_{yy}	−4.5	−1.1	−1.3	−0.6	−0.1
	T_{zz}	14.2	3.6	3.9	4.7	22.5

The cation radical spin distribution has the main components on O2 (0.45), N3 (0.24), and C5 (0.33), whereas for the anion the main portion of the spin is on C6 (0.55), with some smaller components also on N1, N3, and C4. This correlates well with the proton HFCCs, in that the main couplings are on C5−H (cation) and C6−H (anion), respectively. For all atoms, however, the calculated couplings are far from those observed experimentally—including those assigned to the cation in 5′dCMP and the anion in 3′CMP, respectively. We can thus conclude that the radicals observed experimentally are not the

TABLE 3: Calculated Proton Hyperfine Tensors (MHz) of Dehydrogenated Cytosine Radicals

H removed from	HFCC	N1−H	N4−Ha	N4−Hb	C5−H	C6−H
N1	A_{iso}		−2.0	−1.5	−31.5	4.5
	T_{xx}		−1.4	−2.0	−19.2	−3.8
	T_{yy}		−1.0	−1.0	−1.0	0.5
	T_{zz}		2.4	3.0	20.2	3.3
N4 (amino grp)	A_{iso}	−5.9	−43.5		−6.1	1.5
	T_{xx}	−5.2	−34.9		−2.9	−1.6
	T_{yy}	−1.6	−7.9		−1.3	0.0
	T_{zz}	6.8	42.9		4.2	1.6

pure ionic systems but (if formed) have undergone subsequent protonation/deprotonation to form neutral radicals.

B. Dehydrogenation Products. Four dehydrogenation species ("deprotonated cations") are possible, obtained by net removal of a hydrogen from the N1, N4, C5, or C6 positions, respectively. The **N1** species is energetically the most stable, with the **N4** dehydrogenated radical at 2.3 kcal/mol higher energy. The **C6** and **C5** products lie 8.1 and 12.6 kcal/mol above **N1**, respectively. In Table 3, we list the proton hf tensors for the two most stable species only (**N1** and **N4**). In **N1**, which is the most likely dehydrogenation product in, e.g., cytosine monohydrate, the spin displays an alternating pattern with the main components localized primarily on C5 (0.49), O2 (0.35), and N1 (0.29). This matches only in part the estimates from the experimental spectra of the "N1" radical in cytosine monohydrate: 0.57 at C5 and 0.17 at N4 (calculated, 0.02). In the nucleotides, the N1 position connects the base to the sugar moiety, and we may instead expect the **N4** product to be the dominating dehydrogenation species in these cases. In **N4**, the unpaired electron is located almost entirely on the amino nitrogen (0.72) with the remainder on N3 (0.28), although the ring system here also displays an alternating spin pattern.

If we compare the computed hyperfine data for **N1** to that assigned to the "N1" product in cytosine monohydrate,[32] we again note very little similarity between the two. For the main hyperfine tensor, on C5−H, the computed isotropic coupling is 10 MHz too small compared to the experimentally observed data. There is furthermore a very poor match to the assigned amino group protons. Interestingly, not only the isotropic but also the anisotropic components deviate considerably. It is well-known that the main computational difficulties for HFCCs are in obtaining a sufficient fraction of the isotropic coupling constants. This is due to the fact that this component is obtained by summing contributions only at a particular point in space, whereas the anisotropic components are obtained by integrating over all space. The latter generally reproduce 90−95% of the experimental couplings. The deviations we observe here are hence too large to be ascribed to the theoretical method employed. A more likely explanation is that it is not the **N1** radical that has been observed experimentally.

This hypothesis is supported by a more careful investigation of the effects of rotation about the N4−C4 amino bond on the amino proton hyperfine couplings in **N1**. In Figure 1A we show the potential energy curve for the rotation obtained by keeping one proton in a fixed torsional angle at each point and optimizing the position of the second proton as well as all distances and angles in the amino group. As seen there is a clear preference for the proton to be in a nearly in-plane arrangement (with a slight pyramidalization of the nitrogen). The barrier to rotation is very high, ca. 20 kcal/mol, and we can thus expect the amino group to have a more or less fixed orientation. In Figure 1B we show the variations in the full hyperfine tensors (A_{xx}, A_{yy}, A_{zz}, obtained by summing the isotropic coupling with each of the anisotropic components) for the two amino group protons with varying torsional angle. In the arrangements with lowest potential energy, all tensor components lie close to zero (largest value −4.5 MHz). The numerically largest components are observed for the rotational angles of ±120°, corresponding to the transition states on the potential energy surfaces. Even at these points, however, the values of the largest negative couplings, ca. −9 MHz, are only about half of those observed experimentally.

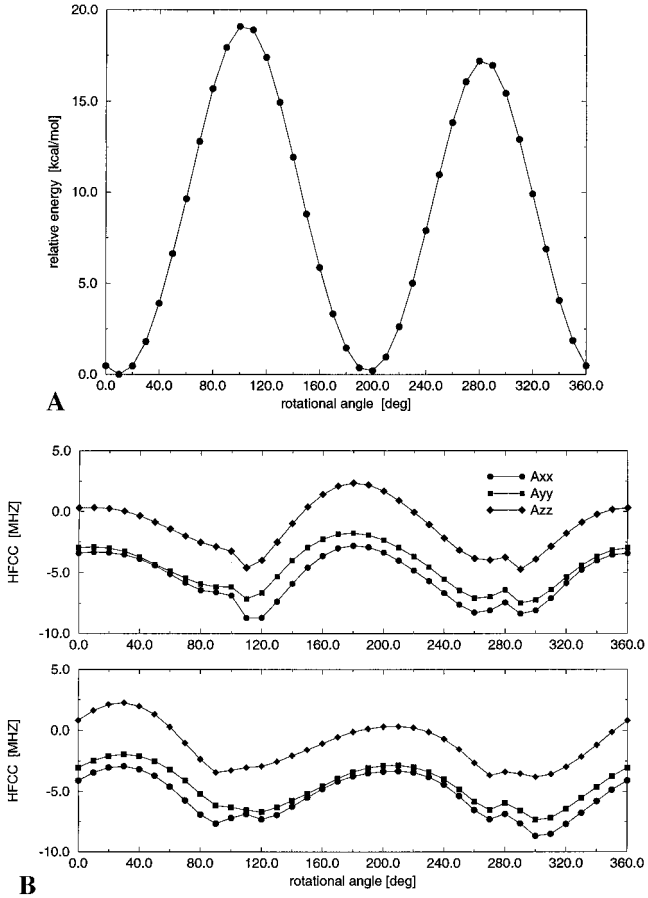

Figure 1. Effects of rotation of the amino group hydrogen in the **N1** dehydrogenation product in cytosine on (A) energy and (B) N4−Ha and N4−Hb hyperfine tensors.

Another possible explanation for the observed spectra could be that hydrogen removal has occurred at the N4 position rather than at N1—possibly owing to a more favorable hydrogen-bonding interaction. However, the calculated HFCCs of the **N4** dehydrogenation product bear very little resemblance to those experimentally assigned to "N1". Instead, fair agreement is noted between the two minor couplings ascribed to the "N3H" adduct of cytosine monohydrate and those computed at the N1 and C5 protons of **N4**. Also, the isotropic component of the remaining amino proton agrees well with that assigned to C5−H in "N1"—the computed anisotropic components for this nucleus are, however, far larger than those observed experimentally. One possible explanation for the deviation between the two sets of numbers could also in this case be a different relative orientation of the N4−H atom, although it is known that rotations of β-protons generally affect the isotropic and not the anisotropic HFCCs. To investigate this hypothesis, we rotated also this system about the C4−N4 bond, reoptimizing the full system at each step. The resulting energy curve is shown in Figure 2A, and Figure 2B displays the full N4−H hyperfine tensor as a function of the rotational angle. The global minimum is at a

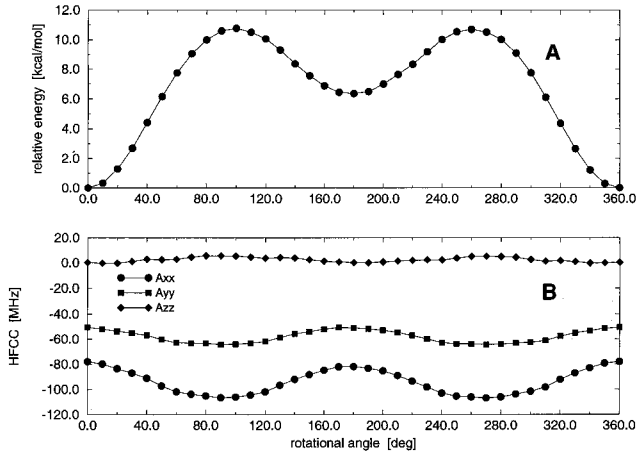

Figure 2. Effects of rotation of the amino hydrogen in the **N4** dehydrogenation product in cytosine on (A) energy and (B) N4−H hyperfine tensor.

TABLE 4: Calculated Proton Hyperfine Tensors (MHz) of Hydrogenated Cytosine Radicals

H added to	HFCC	N1−H	N4−Ha	N4−Hb	C5−H	C6−H	H-add
N3	A_{iso}	−8.5	55.0	−3.2	4.9	−38.4	1.8
	T_{xx}	−7.9	−2.9	−4.3	−4.6	−23.4	−7.0
	T_{yy}	−3.5	−2.7	−1.4	1.8	0.5	−2.9
	T_{zz}	11.4	5.6	5.7	2.8	22.9	9.9
O2	A_{iso}	−2.4	11.3	6.8	2.2	−34.3	−0.4
	T_{xx}	−8.7	−4.4	−4.3	−4.3	−24.6	−1.5
	T_{yy}	−3.6	−2.2	−2.5	1.4	1.0	−1.3
	T_{zz}	12.3	6.6	6.8	2.9	23.7	2.8
C5	A_{iso}	−9.8	0.7	0.0	124.9	−39.7	39.2
	T_{xx}	−8.9	−0.8	−1.1	−3.5	−30.2	−4.5
	T_{yy}	−4.6	−0.7	−0.9	−3.0	−0.9	−3.6
	T_{zz}	13.5	1.5	2.0	6.5	31.1	8.1
C6	A_{iso}	−3.5	−2.7	−2.7	−45.9	126.4	117.7
	T_{xx}	−2.5	−2.1	−3.1	−28.5	−4.5	−4.3
	T_{yy}	−2.2	−1.5	−1.5	−1.3	−2.6	−2.6
	T_{zz}	4.7	3.6	4.6	29.8	7.1	6.9

rotational angle of 0°, i.e., with the hydrogen lying in the plane of the ring and pointing toward N3. The barrier toward rotation is again rather high, ca. 12.6 kcal/mol, with transition states at orientations perpendicular to the ring and with an energetically high-lying local minimum for the hydrogen located in the ring plane at a 180° rotational angle (pointing toward C5−H).

The HFCCs of the amino proton vary somewhat with rotational angle. The changes are, however, relatively small and in the opposite direction to those required in order to reproduce the observed full tensor couplings of (−63, −42, −20) MHz. On the basis of this analysis we may hence also discard the ionized moiety, subsequently deprotonated at the amino group, as being observed in the irradiated sample. The proposed net reaction of radiation-induced electron transfer between the cytosines followed by proton transfer from N1 (or N4) of the cationic cytosine unit to N3 of the anionic cytosine thus seems incorrect. We also note that no net dehydrogenation products have been reported in the larger cytosine derivatives. However, as no hydrogen-bonded base pairs were investigated in this work, we cannot rule out the possibility of proton transfer from, e.g., C to G, in the full DNA samples.

C. Hydrogen Adducts. The next set of radicals investigated are the possible hydrogenation products ("protonated anions"). Four possible products were studied, formed via electron uptake plus proton addition to either O2, N3, C5, or C6 positions (Table 4). The energetically lowest lying species is that where net H addition occurs at the N3 position (**N3H**), whereas the other three lie between 8 (**C5H**) and 14 (**O2H**) kcal/mol higher in energy. For the **N3H** product, the main spin components are at the C6 (0.53) and O4 (0.37) positions. The reported experimental estimates for the spin distribution in cytosine monohydrate are 0.52 at C5, 0.07 at N3, and 0.06 at N4.[26] The calculated data for the latter two spin densities are 0.09 at N3 and 0.03 at N4. For the two carbon hydrogen addition products, the unpaired electron is primarily localized to the neighboring carbon atom such that **C5H** has a spin of 0.74 on C6 and **C6H** has a spin population of 0.75 on C5. The values estimated by Sagstuen et al. in cytosine monohydrate are 0.74 at C5 in **C6H** and 0.72−0.74 at C6 in **C5H**, in close agreement with the computed data. For the **O2H** adduct, finally, the main fraction of the unpaired spin is located on the C6 carbon (0.56) and the C4 carbon (0.31). This is considerably larger than the estimated value at C6 for the assumed room-temperature "O2H" adduct observed by Herak et al. (0.36).[44]

The HFCCs of the **N3H** adduct, displayed in Table 4, show reasonable agreement with those observed experimentally. The components of the largest tensor, at C6−H, are at the most 1.8 MHz off. The tensor assigned to one of the amino protons, (−9, −7, 2) MHz, is in reasonable agreement with the computed data for one of the N4 hydrogens, (−8, −5, 3) MHz. The difference is most likely due to a small rotation about the C4−N4 bond, possibly stabilized via hydrogen bonding in the crystal. As seen from the computed HFCCs, the second amino proton carries a very large isotropic component (55 MHz)—it may appear somewhat odd that this has not been observed in the experimental studies. However, assuming that the amino group is slightly rotated (cf. above), the isotropic value of this proton should also be modified.

The **O2H** adduct also displays a large tensor at the C6 hydrogen, which closely resembles that of the **N3H** adduct. The remaining couplings differ more from the experimental ones, and it may be concluded that this radical is probably not observed in cytosine monohydrate. The couplings observed at room temperature and assigned to this system (A_{iso}, −27 MHz; anisotropic components, −15, 2, 14 MHz) could not be traced to any of the computed values for **O2H**—nor for any other of the many radicals investigated in this work except possibly the C5−H proton of the cation. For these systems, however, the calculated and experimental spin distributions deviate considerably (see above). One further, although less likely, possibility could be that for the case of **O2H** the high temperature causes vibrational averaging or ring-puckering effects, not accounted for in the present study. We also note that the calculated C6−H hf splitting of the **O2H** radical matches well with the main computed and experimental tensors of "N3H" in the various systems and also the "anion" radical in 3′CMP.

Both **C5H** and **C6H** are nonplanar, as the hydrogen addition causes a slight ring-puckering. The two protons on the carbon subjected to addition reaction are hence placed asymmetrically with respect to the ring plane (pseudoaxially and pseudoequatorially) and display nonequivalent hf tensors (Table 4). The largest differences are observed for the **C5H** adduct. Sagstuen et al. assigned the two β-protons with $A_{iso} = 132$ and 87 MHz to the "C5H" adduct, along with the tensor at C6−H of $A_{iso} = -52.4$ MHz, $T_{ii} = (-32, 2, 30)$ MHz. A second α-proton tensor was also observed, with $A_{iso} = -51.8$ MHz and $T_{ii} = (-28, 0, 28)$ MHz, which was assigned to C5−H in the "C6H" adduct. In 1-methylcytosine the two "C5H" and "C6H" adducts have also been observed (Table 1), displaying similar tensors as those in cytosine monohydrate. From the data of Table 4, we note a slightly closer agreement with the data for the α-proton tensors

TABLE 5: Calculated Proton Hyperfine Tensors (MHz) of Hydroxylated Cytosine Radicals

OH add to	HFCC	N1−H	N4−Ha	N4−Hb	C5−H	C6−H	H−O
C5	A_{iso}	−11.7	−0.2	−0.2	92.5	−29.8	−0.3
	T_{xx}	−9.9	−1.0	−0.9	−4.5	−27.0	−7.1
	T_{yy}	−4.9	−0.6	−0.8	−1.4	−0.8	−0.2
	T_{zz}	14.8	1.6	1.7	5.9	27.8	7.3
C5-2	A_{iso}	−10.7	−0.3	−0.3	104.9	−37.3	−1.7
	T_{xx}	−9.0	−0.4	−1.2	−4.2	−28.7	−2.7
	T_{yy}	−4.8	−0.3	−0.8	−2.2	−0.9	−2.2
	T_{zz}	13.8	0.7	2.0	6.4	29.6	4.9
C6	A_{iso}	0.5	−3.7	−2.7	−49.2	36.6	13.5
	T_{xx}	−2.1	−2.2	−3.8	−29.9	−4.6	−3.2
	T_{yy}	−0.2	−1.7	−1.7	−1.4	−2.9	−1.7
	T_{zz}	2.3	3.9	5.5	31.3	7.5	4.9

in **C6H** than in **C5H**. The calculated isotropic β-couplings are 125 and 39 MHz in **C5H** and 126 and 118 MHz in **C6H**, respectively. The deviation from the observed couplings can be ascribed to an insufficient ring puckering obtained in these two systems, and thereby sufficiently large hf tensors are not obtained. The anisotropic tensors, however, match very closely those observed experimentally for all the nuclei, and it seems clear that the calculations on **C5H** and **C6H** support the assignments made for the corresponding systems in C and 1MeC.

D. OH Addition Products. The final radicals investigated in the present work are those arising from net OH radical attack at the C5 and C6 carbons (Table 5). The two adducts lie relatively close in energy, with **C6OH** ca. 2.4 kcal/mol less stable than **C5OH**. For the **C5OH** adduct, we also observed a second species (**C5OH-2**), with a different torsional orientation of the amino group relative to the added OH group and the ring plane, which lies ca. 0.6 kcal/mol above the **C6OH** adduct. Similar to the case of the corresponding hydrogen adducts, the main part of the unpaired spin density is located on the neighboring (C6/C5) carbon, with values of 0.70 on C6 in **C5OH** and 0.78 on C5 in **C6OH**. The large spin density on the adjacent carbon results in a large induced hf tensor on the α-hydrogen bonded to it. Since the spin densities are highly similar to the net hydrogen adducts, the corresponding proton couplings are also similar (cf. the C6−H tensor in **C5H** and **C5OH**, and the C5−H tensor in **C6H** and **C6**−**OH**). In analogy with the H-adducts, the rings undergo puckering distortion also for the OH adducts. The OH group thereby attains the pseudoequatorial position, leading to large hf tensors for the β-proton in an axial position (see below). Unsuccessful attempts were made to locate conformers with the β-proton in an equatorial arrangement.

As seen from Table 5, the HFCCs of the two **C5OH** adducts vary by up to 13 MHz, especially for the C5−C6 fragments, despite the relatively small geometric differences (i.e., a change in rotational angle about the C4−N4 bond). We also note that the N1−H couplings of **C5OH** are those in the entire computed set that best fits those assigned to the amino protons in "N1". There is one large negative isotropic component (−30 to −50 MHz), at C6−H in **C5OH** and at C5−H in **C6OH**. This also agrees with the large negative coupling of −41 MHz in "N1", although the corresponding anisotropic data show larger deviations. A large positive coupling is also noted for the out-of-plane hydrogen C5−H in the C5 hydroxy adducts, that might prove a valuable distinguishing "fingerprint" for this particular radical. The corresponding isotropic coupling for the C6−H proton in **C6OH** is, albeit large and positive, considerably smaller.

Discussion and Conclusions

One main conclusion from our calculations is that there are several radicals possible and that many seem to have radical centers with highly similar hyperfine tensors. A full understanding of the reaction products in irradiated cytosine or its derivatives thus by necessity requires experimental identification and analysis of as many other proton couplings in the sample as possible (as well as nitrogen couplings and, possibly, ^{13}C- and/or ^{17}O-labeled samples). In several of the cytosine derivatives, the **N3H** hydrogenation adduct seems to be present. However, in none of the experimental studies do we find reports of a nearly isotropic tensor centered around 55 MHz, a set that calculations show to be present in this system only and that hence could facilitate a unique identification of the **N3H** radical. Although the identification of the different radical centers is reasonably clear, several ambiguities still prevail. In, e.g., 1MeC, we note that there are as many as three hydrogen adducts identified (**N3H**, **C5H**, and **C6H**). But where do these hydrogens come from? If they are generated within the samples, then dehydrogenation products must also be present. No such products have, however, as yet been reported experimentally.

Through the comparisons between theory and experiment, we have been able to show that the charged radical anion and cation of cytosine have not been directly detected to date. The "cation" of 5′dCMP and the "anion" of 3′CMP can instead, in both cases, be assigned to the **N3H** adducts, possibly in different local environments leading to slightly modified hf tensors. One possible explanation for this (see below) may be that the charged radicals are not stable for sufficiently long periods of time to be detectable but quickly undergo protonation, deprotonation, hydration, and similar reactions. We have also been able to positively rule out the room-temperature "O2H" cytosine adduct,[44] unless accompanied by significant vibrational motion.

In cytosine monohydrate, the assumptions made by Sagstuen et al.[26] are correct from an energetic point of view in that the lowest lying forms within the dehydrogenation and hydrogenation classes correspond to the net reaction whereby N1−H of one cytosine has migrated to the N3 position of a neighboring molecule. There is also, as commented earlier, a satisfactory agreement for the HFCCs of the **N3H** hydrogenated radical (Tables 1 and 4), although possibly associated with a slightly modified torsional angle about the amino group by means of hydrogen bonding. For the **N1** dehydrogenated species, however, the calculated hyperfine structures show very little resemblance to those observed experimentally. In fact none of the charged or net hydrogenation/dehydrogenation products fits the hf structure of "N1". We have also modeled several different systems with hydrogen bonding—not explicitly reported in this work—with up to four water molecules, adding various neighboring cytosine fragments or even the singlet/triplet cytosine dimer in order to model the **N1**−**N3H** diradical pair. None of these have yielded results that would support **N1** as a possible candidate for the observed spectrum. We furthermore note that for the large couplings of the C5 and the N1 protons in **C5OH** and **C5OH-2** there is a fair match with the experimental sets assigned to "N1". We may also tentatively assign the two tensors ascribed to N4−H of "N1" to the N1−H proton in the two different geometric conformers **C5OH** and **C5OH-2**. This would explain the presence of these sets of couplings in the smaller cytosine system but not in any of the larger derivatives in which the N1−H is replaced by a methyl group or sugar moiety.

From the hyperfine data, it thus seems that the main net products in irradiated cytosine monohydrate are the **N3H** and

C5OH adducts. At least three possible mechanisms can be considered, leading to either **N3H** + **N1** or **N3H** + **C5OH**. In the first of these, only the cytosines are involved, such that one unit is ionized (the electron of which is captured by another unit), followed by deprotonation of the cation and protonation of the anion:

$$\mathrm{Cyt} + \mathrm{Cyt} \rightarrow \mathrm{Cyt}^+ + \mathrm{Cyt}^- \rightarrow \mathbf{N1} + \mathbf{N3H} \qquad (1)$$

The energetics at the B3LYP/6-311G(2df,p) level (on B3LYP/6-31G(d,p) optimized geometries) is +207 kcal/mol for the electron-transfer step and −139 kcal/mol for the proton-transfer reaction. The overall process is endothermic by 68 kcal/mol. The second and third mechanisms both involve water molecules and lead to the formation of the **C5OH** product rather than **N1.** In the first of these, ionization and electron uptake is assumed to occur on the cytosines, as above, but where water subsequently adds to the cation, followed by deprotonation/proton transfer to the anion:

$$\mathrm{Cyt} + \mathrm{Cyt} + \mathrm{H_2O} \rightarrow \mathrm{Cyt}^+ + \mathrm{Cyt}^- + \mathrm{H_2O} \rightarrow \mathbf{C5OH} + \mathbf{N3H} \qquad (2)$$

The energetics of the first step is the same as in eq 1, +207 kcal/mol, whereas for the second reaction we gain 149 kcal/mol; the overall net energy cost is 58 kcal/mol. In the third mechanism, ionization of water is assumed to occur, leading to the water cation and the cytosine anion. The water cation then decomposes into a proton and an OH radical, which add to the cytosine anion and a neutral cytosine unit, respectively:

$$\mathrm{H_2O} + \mathrm{Cyt} + \mathrm{Cyt} \rightarrow \mathrm{H_2O}^+ + \mathrm{Cyt} + \mathrm{Cyt}^- \rightarrow \mathbf{C5OH} + \mathbf{N3H} \qquad (3)$$

Since this reaction has the same initial and final points as eq 2, the net reaction energy (+58 kcal/mol) is the same. The intermediate step is, however, more endothermic (+298 kcal/mol) and the subsequent decomposition of the water cation plus addition reactions more exothermic (−240 kcal/mol) than the corresponding intermediate steps in eq 2.

Of the three mechanisms outlined above, the second one, involving electron transfer, hydration of the cation, and proton transfer to the anion is probably the most likely to occur. First of all, on the basis of the number of electrons in cytosine relative to water, it can be estimated that 85% of the radiation-induced ionization processes should occur on cytosine. Second, similar reaction processes have been observed in thymine.[46] And, of the three mechanisms, it is the one with the lowest endothermicities involved in the initial ionization step and in the overall process.

On the other hand, the third mechanism, radiolysis of water to produce OH radicals and OH radical adducts, is a commonly employed technique in ESR spectroscopy.[2,8,10,47,48] In recent studies by Sevilla and co-workers on DNA samples with varying degrees of hydration, metastable OH radicals were observed in the intermediate hydration shell.[47] No OH radicals were observed in the closest hydration layer, however, which was taken as an indication of hole transfer to DNA. It has also been speculated that this is due to the fact that the OH radicals generated near the sample may readily react with it, and the present work may be taken as an indication that further, more detailed studies are needed in order to clearly rule out the latter option. Hütterman et al.[49] have presented evidence for the dependence of radical formation on water concentration. Their study indicated that the larger the number of water molecules in the hydration layer of DNA, the more radicals are formed. In addition, Wala et al.[50] have reported on OH-induced strand breakage of DNA, caused by OH addition to a base. Upon exposure of DNA to OH radicals, deamination is known to occur at the cytosine base, as well as the formation of 5-hydroxycytosine,[51] and OH radical adducts have been well-established in irradiated frozen aqueous solutions of deoxyadenosine[52] and guanine hydrobromide monohydrate.[53]

On the basis of the overall findings in these latter studies it seems reasonable to assume that a hydroxylated product could be formed also in irradiated cytosine monohydrate, and the present calculations support such a hypothesis. We also note that in the crystalline samples of the larger cytidine derivatives, only hydrogenation adducts have thus far been positively identified—possibly the present study can assist in the identification of OH adducts also in those crystalline monohydrates. We finally stress that the present calculations are performed in vacuum and that effects of the local environment were not taken into account in the present work.

Acknowledgment. Financial support from the Swedish Natural Sciences Research Council (NFR), the Natural Sciences and Engineering Research Council of Canada (NSERC), and the Killam Trust are gratefully acknowledged. We also acknowledge generous grants of computer time from the National Supercomputing Center (NSC) in Linköping and from the Center for Parallel Computing (PDC) in Stockholm.

References and Notes

(1) Hüttermann, J., Köhnlein, R., Teoule, R., Bertinchamps, A. J., Eds. *Effects of Ionizing Radiation on DNA*; Springer-Verlag: Heidelberg, 1978.

(2) von Sonntag, C. *The Chemical Basis of Radiation Biology*; Taylor and Francis: London, 1987.

(3) von Sonntag, C.; Schuchmann, H.-P. *Int. J. Radiat. Biol.* **1986**, *49*, 1 and references therein.

(4) Hüttermann, J. In *Radical Ionic Systems*; Lund A., Shiotani, M., Eds.; Kluwer Academic: Boston, MA, 1991; p 435.

(5) Close, D. M. *Radiat. Res.* **1993**, *135*, 1.

(6) Heelis, P. F.; Hartman, R. F.; Rose, S. D. *Chem. Soc. Rev.* **1996**, 289.

(7) Cadet, J.; Vigny, P. In *Bioorganic Photochemistry, Photochemistry and the Nucleic Acids*; Morrison, H., Ed.; Wiley: New York, 1990; Vol. 1, p 1.

(8) Dizdaroglu, M.; Gajewski, E.; Reddy, P.; Margolis, S. A. *Biochemistry* **1989**, *28*, 3625.

(9) Olinski, R.; Briggs, R. C.; Hnilica, L. S.; Stein, J.; Stein, G. *Radiat. Res*. **1981**, *86*, 102.

(10) Gajewski, E.; Dizdaroglu, M. *Biochemistry* **1990**, *29*, 977 and references therein.

(11) Colson, A. O., Sevilla, M. D. *Int. J. Radiat. Biol*. **1995**, *67*, 627.

(12) Paglieri, L.; Corogniu, G.; Estrin, D. A. *Int. J. Quantum Chem*. **1995**, *56*, 615.

(13) Hutter, M.; Clark, T. *J. Am. Chem. Soc.* **1996**, *118*, 7574.

(14) Sponer, J.; Hobza, P. *Int. J. Quantum Chem.* **1996**, *57*, 959.

(15) Andzelm, J. A.; Wimmer, E. *J. Chem. Phys.* **1992**, *96*, 1280. Johnson, B. G.; Gill, P. W. M.; Pople, J. A. *J. Chem. Phys.* **1993**, *98*, 5612. Bauschlicher, C. W., Jr.; *Chem. Phys. Lett.* **1995**, *246*, 40.

(16) *Density Functional Methods in Chemistry*; Labanowski, J., Andzelm, J., Eds.; Springer-Verlag: New York, 1993. *Theoretical and Computational Chemistry, Vol. 2, Modern Density Functional Theory—A Tool for Chemistry*; Politzer P., Seminario, J. M., Eds.; Elsevier: New York, 1995. *Recent Advances in Density Functional Theory, Parts 1 and II*; Chong D. P., Ed.; World Scientific: Singapore, 1995. *Density Functional Methods in Chemistry and Materials Sciences*; Springborg, M., Ed.; Wiley: New York, 1997.

(17) Himo, F.; Gräslund, A.; Eriksson, L. A. *Biophys. J.* **1997**, *72*, 1556.

(18) Himo, F.; Eriksson, L. A. *J. Phys. Chem.* **1997**, *B101*, 9811.

(19) Himo, F.; Eriksson,. L. A., *J. Chem. Soc., Perkin Trans. 2* **1998**, *2*, 305.

(20) Lassmann, G.; Eriksson, L. A.; Himo, F.; Lendzian, F.; Lubitz, W. **1998**, submitted.

(21) Eriksson, L. A.; Himo, F.; Siegbahn, P. E. M., Babcock, G. T. *J. Phys. Chem.* **1997**, *A101*, 9496.

(22) Wetmore, S. D.; Boyd, R. J.; Eriksson, L. A. *J. Phys. Chem.* **1998**, *B102*, 5369.
(23) Eriksson, L. A.; Himo, F. *Trends Phys. Chem.*, **1997**, *6*, 153.
(24) Himo, F.; Eriksson, L. A. *J. Am. Chem. Soc.* **1998**, in press.
(25) Siegbahn, P. E. M.; Eriksson, L. A.; Himo, F.; Pavlov, M. **1998**, submitted.
(26) Sagstuen, E.; Hole, A. O.; Nelson, W. H.; Close, D. M. *J. Phys. Chem.* **1992**, *96*, 8269.
(27) Weber, H. P.; Craven, B. M.; McMullan, R. K. *Acta Crystallogr.* **1980**, *B36*, 645. McClure, R. J.; Craven, B. M. *Acta Crystallogr.* **1973**, *B29*, 1234.
(28) Rustgi, S. N.; Box, H. C. *J. Chem. Phys.* **1974**, *60*, 3343. Close, D. M.; Bernhard, W. A. *Bull. Am. Phys. Soc.* **1980**, *25*, 416.
(29) Box, H. C.; Potter, W. R.; Budzinski, E. E. *J. Chem. Phys.* **1975**, *62*, 3476.
(30) Close, D. M.; Bernhard, W. A. *J. Chem. Phys.* **1979**, *70*, 210.
(31) Slater, J. C. *Quantum Theory of Molecules and Solids*; McGraw-Hill: New York, 1974.
(32) Becke, A. D. *Phys. Rev.* **1988**, *A38*, 3098.
(33) Vosko, S: H.; Wilk, L.; Nusair, M. *Can. J. Phys.* **1980**, *58*, 1200.
(34) Lee C.; Yang W.; Parr R. G. *Phys. Rev. B* **1988**, *37*, 785.
(35) Becke A. D. *J. Chem. Phys.* **1993**, *98*, 1372.
(36) Perdew J. P.; Wang Y.. *Phys. Rev. B* **1986**, *33*, 8800.
(37) Perdew J. P. *Phys. Rev. B* **1986**, *33*, 8822; **1986**, *34*, 7406.
(38) Frisch, M. J.; Trucks, G. W.; Schlegel, H. B.; Gill, P. M. W.; Johnson, B. G.; Robb, M. A.; Cheeseman, J. R.; Keith, T. A:; Peterson, G. A.; Montgomery, J. A.; Raghavachari, K.; Al-Laham, M. A.; Zakrewski, V. G.; Ortiz, J. V.; Foresman, J. B.; Cioslowski, J.; Stefanov, B. B.; Nanayakkara A.; Challacombe, M.; Peng, C. Y.; Ayala, P. Y.; Chen, W.; Wong, M. W.; Andres, J. L.; Replogle, E. S:; Gomperts, R.; Martin, R. L.; Fox, D. J.; Binkley, J. S.; DeFrees, D. J.; Baker, J.; Stewart, J. P.; Head-Gordon, M.; Gonzalez, C.; Pople, J. A. *Gaussian 94*; Gaussian Inc.: Pittsburgh, PA, 1995.
(39) St-Amant, A.; Salahub, D. R. *Chem. Phys. Lett.* **1990**, *169*, 387. St-Amant, Ph.D. Thesis, Université de Montreal, 1991. Salahub, D. R.; Fournier, R.; Mlynarski, P.; Papai, I.; St-Amant, A.; Ushio, J. In *Density Functional Methods in Chemistry*; Labanowski, J., Andzelm, J., Eds.; Springer-Verlag: New York, 1993.
(40) Eriksson, L. A. *Mol. Phys.* **1997**, *91*, 827.
(41) Malkin, V. G.; Malkina, O. L.; Eriksson, L. A.; Salahub, D. R. In *Theoretical and Computational Chemistry, Vol. 2, Modern Density Functional Theory—A Tool for Chemistry*; Politzer P., Seminario, J. M., Eds.; Elsevier: New York, 1995; p 273.
(42) Barone, V. In *Recent Advances in Density Functional Theory*; Chong D. P., Ed.; World Scientific: Singapore, 1995; Part 1, p 287.
(43) Engels, B.; Eriksson, L. A.; Lunell, S. *Adv. Quantum Chem.* **1997**, *27*, 298.
(44) Herak, J. N.; Lenard, D. R.; McDowell, C. A. *J. Magn. Reson.* **1977**, *26*, 189.
(45) Orlov, V. M.; Smirnov, A. N.; Varshavsky, Y. M. *Tetrahedron Lett.* **1976**, *48*, 4377.
(46) Decarroz, et al. *Int. J. Radiat. Biol.* **1986**, *50*, 491.
(47) Becker, D.; La Vere, T.; Sevilla, M. D. *Radiat. Res.* **1994**, *140*, 123. LaVere, T.; Becker, D.; Sevilla, M. D. *Radiat. Res.* **1996**, *145*, 673.
(48) Hiraoka, W.; Kuwabara, M.; Sato, F.; Matsuda, A.; Ueda, T. *Nucleic Acids Res.* **1990**, *18*, 1217.
(49) Hüttermann, J.; Röhrig, M.; Köhnlein, W. *Int. J. Radiat. Biol.* **1992**, *61*, 299.
(50) Wala, M.; Bothe, E.; Görner, H.; Shulte-Frohlinde, D. *J. Photochem. Photobiol. A* **1990**, *53*, 87.
(51) Chapman, D.; Gillespie, C. J. *Adv. Radiat. Biol.* **1981**, *9*, 143. Téoule, R. *Int. J. Radiat. Biol.* **1987**, *51*, 573.
(52) Gregoli, S.; Olast, M.; Bertinchamps, A. *Radiat. Res.* **1974**, *60*, 388.
(53) Hole, E.; Sagstuen, E.; Nelson, W. H.; Close, D. M. *Radiat. Res.* **1991**, *125*, 119.